Influence of the Properties of a Glass Fiber Reinforced Polymer Deck on the Dynamic Response of a Road Bridge

Gallegos-Calderón, Christian [1,2,*] ; **Oliva-Quecedo, Javier** [2] ; **Pulido, M. Dolores G.** [1,3] ; **Goicolea, José M.** [1]

[1] *Universidad Politécnica de Madrid, E.T.S.I. Caminos, Canales y Puertos, Madrid, España*
[2] *AR2V Ingeniería, Madrid, España*
[3] *Instituto de Ciencias de la Construcción Eduardo Torroja CSIC, Madrid, España*

Abstract: The use of multicellular Glass Fiber Reinforced Polymer (GFRP) deck panels in the rehabilitation and construction of bridges has increased over the last 30 years due to several benefits, such as: low maintenance cost, fast installation, corrosion resistance, and high strength-to-weight ratio. Due to the orthotropic nature of GFRP decks and their complex cross-section geometry, expensive computational problems may be obtained when bridges that include these elements are analyzed under traffic loads. Therefore, this paper studies the dynamic response of a GFRP-steel road bridge modelling the multicellular GFRP deck as an orthotropic plate. For this purpose, a finite element model of the hybrid structure is developed, and a sensitivity analysis is carried out to investigate the influence of the mechanical properties of the orthotropic element on the bridge behavior. The roughness of the pavement, the degree of composite action between the deck and the stringers, the multibody dynamic model of a truck, and the vehicle-bridge interaction phenomenon are included in the analyses. Results indicate that the most relevant properties of the orthotropic plate on the response of the structure are the modulus of elasticity in the longitudinal direction, the modulus of elasticity in the transverse direction, and the shear modulus. Also, achieving a full composite action and avoiding deterioration of road are identified as key aspects to reduce the vibration levels on the hybrid bridge.

Keywords: GFRP-steel bridge, dynamic response, road roughness, vehicle-bridge interaction

Influencia de las Propiedades de un Tablero de Polímero Reforzado con Fibra de Vidrio en la Respuesta Dinámica de un Puente Carretero

Resumen: El uso de tableros multicelulares de Polímero Reforzado con Fibra de Vidrio (GFRP por sus siglas en inglés) en la rehabilitación y construcción de puentes ha aumentado en los últimos 30 años por varios motivos, como: el bajo costo de mantenimiento, rápida instalación, resistencia a la corrosión, y alta relación resistencia-peso. Debido a la naturaleza ortotrópa de los tableros de GFRP y la compleja geometría de su sección transversal, el análisis dinámico de puentes que incluyan este tipo de elementos puede representar un problema computacional costoso. Por lo tanto, este artículo estudia la respuesta dinámica de un puente carretero de GFRP-acero cuando se modela el tablero multicelular de GFRP como una placa ortótropa. Para ello, se desarrolla un modelo de elementos finitos del puente híbrido, y se realiza un análisis de sensibilidad para investigar la influencia de las propiedades mecánicas del elemento ortótropo en el comportamiento del puente. La rugosidad del pavimento, el grado de acción compuesta entre el tablero y los largueros, el modelo dinámico multicuerpo de un camión, y la interacción vehículo-puente se tienen en cuenta en el análisis. Los resultados indican que las propiedades más relevantes de la placa ortótropa en la respuesta de la estructura son el módulo de elasticidad en la dirección longitudinal, el módulo de elasticidad en la dirección transversal, y el módulo de cortante. De igual manera, se determina que lograr una acción compuesta total y evitar el deterioro de la vía son aspectos importantes para reducir la respuesta del puente híbrido.

Palabras claves: Puente de GFRP-acero, respuesta dinámica, rugosidad del pavimento, interacción vehículo-puente

*christian.gallegos@upm.es
Recibido: 28/10/2022
Aceptado: 27/04/2023
Publicado en línea: 01/08/2023
10.33333/rp.vol52n1.08

1. INTRODUCTION

Glass Fiber Reinforced Polymer (GFRP) decks are still considered novel applications in Civil Engineering. Nevertheless, these elements have been increasingly used in the rehabilitation and construction of road bridges due to several benefits such as: low maintenance cost, dead load reduction, electromagnetic transparency, fast installation, corrosion resistance, and high strength-to-weight ratio. According to Mara et al. (2014), FRPs also offer sustainable solutions in bridge projects, reducing environmental impact and leading to potential cost savings over the life cycle of a structure. For instance, it has been estimated that carbon emissions could be reduced by 48 % if a GFRP is used instead of concrete for the superstructure of a 12 m long road bridge (Resins, 2009). A comprehensive review about the structural performance of FRP decks for road bridges can be found in Mara and Haghani (2015).

Among the different types of GFRP deck systems, pultruded panels are the most common since their manufacturing process is automated, allowing mass production of the elements and cost savings. As a result, several road bridges around the world have incorporated these panels (Lee et al., 2010; Joint Research Centre, 2016; Kim, 2019). The inherent lightweight nature of GFRP panels is a major advantage over conventional concrete or steel bridge decks, but it may lead to excessive vibrations induced by traffic loading (Aluri et al., 2005; Zhang et al., 2006). In addition, the structural response can be exacerbated by the road surface condition (Oliva et al., 2013) and the degree of composite action between the main girders and the deck (Wan et al., 2005). Therefore, the dynamic performance of a bridge with GFRP elements should be properly assessed considering these parameters. Modeling and analyzing the response of hybrid bridges that include pultruded decks may lead to computationally expensive problems due to two main factors. The first aspect is the complex geometry of the cross-section, which is generally a multicellular hollow profile. Whilst the second reason is that webs and flanges, also known as laminates, of the profiles may present different mechanical properties.

Hence, this paper investigates the response of a hybrid GFRP-steel road bridge under the action of a vehicle when a multicellular deck system is modelled as an orthotropic plate with equivalent elastic properties. For this purpose, a Finite Element (FE) model of the bridge described by Keelor et al. (2004) is developed, and a sensitivity analysis is carried out to study the influence of the mechanical properties of the orthotropic element on the bridge behavior. For the analyses, the H20-44 truck, described in AASHTO (2012), is modeled as a multibody dynamic model to account for the Vehicle-Bridge Interaction (VBI) phenomenon. Also, the irregularities of the pavement together with the degree of composite action between the GFRP plate and the steel stringers are considered.

After this introduction, the paper is organized as follows. In Section 2, the GFRP-steel bridge is described, and the equivalent elastic properties to model the multicellular deck as an orthotropic plate are introduced. The FE model of the road bridge and results from a static analysis are presented in Section 3. In Section 4, modeling the road surface, the multibody dynamic vehicle, and VBI are explained. A sensitivity analysis varying the properties of the orthotropic plate is carried out in Section 5. In Section 6, the bridge dynamic response is discussed in terms of the vehicle speed, the degree of composite action, and the road surface quality. Finally, conclusions are drafted in Section 7.

2. GFRP-STEEL ROAD BRIDGE

In this section, the GFRP-steel bridge is described. Also, expressions to obtain equivalent elastic properties to model a multicellular profile panel as an orthotropic plate are presented.

2.1 Description

The Boyer Bridge, described by Keelor et al. (2004) and analyzed in this work, is a simply supported road bridge with a length L_b of 12.95 m and width of 7.92 m (Figure 1a). The clear span of the bridge is 12.65 m, and the superstructure consists of GFRP pultruded panels placed onto five galvanized steel stringers W610X155 Grade 345. These stringers are laterally restrained by C310x37 steel elements. The deck system, comprised of multicellular profile panels, is connected to the steel stringers by shear studs. Two studs are welded every 0.61 m along the length of the top flange of each stringer, and grout is poured along a haunch with a depth of 12.70 mm at the deck-girder interfaces. Finally, a 0.102 m layer of asphalt over the GFRP panels works as a wearing surface.

2.2 Orthotropic plate

Based on the proposal by Qiao et al. (2000), a multicellular deck system can be considered as an orthotropic plate with equivalent elastic properties using the following expressions:

$$(E_x)_p = 12\frac{D_x}{t_p^3 b_p}(1-\nu_{xy}\nu_{yx}) \tag{1}$$

$$(E_y)_p = 12\frac{D_y}{t_p^3 l_p}(1-\nu_{xy}\nu_{yx}) \tag{2}$$

$$\frac{\nu_{xy}}{D_x} = \frac{\nu_{yx}}{D_y} \tag{3}$$

$$(G_{xy})_p = 6\frac{D_{xy}}{t_p^3} \tag{4}$$

$$(G_{xz})_p = \frac{F_x}{t_p b_p} \tag{5}$$

$$(G_{yz})_p = \frac{F_y}{t_p l_p} \tag{6}$$

where D_x and D_y are the bending stiffness of the cellular deck in x and y direction, respectively, F_x and F_y are the out-plane shear stiffness in x and y direction, D_{xy} is the torsional stiffness per unit width, t_p is the thickness of the plate, b_p is the width of the plate, l_p is the length of the plate, ν_{xy} is the Poisson's ratio, n_c is the total number of cells, and b is the width of a single cell.

Equations (1)-(6) are employed considering that the GFRP panels of the Boyer Bridge have the same geometry and mechanical properties of those used in the S655 Bridge. Information about the deck, whose cross-section is shown in Figure 1b, can be found in Wan et al. (2005). Additionally, for the calculation, $b_p = 12.95$ m and $l_p = 7.92$ m are adopted. Table 1 presents the equivalent properties of the orthotropic plate.

Table 1. Equivalent properties of the orthotropic plate

Parameter	Symbol	Units	Value
Density	ρ_p	kg/m^3	480
Thickness	t_p	m	0.195
Modulus of elasticity in x dir.	$(E_x)_p$	GPa	15.63
Modulus of elasticity in y dir.	$(E_y)_p$	GPa	7.16
In-plane Poisson's ratio	ν_{xy}	-	0.30
In-plane shear modulus	$(G_{xy})_p$	GPa	6.45
Out-plane shear modulus xz	$(G_{xz})_p$	GPa	0.88
Out-plane shear modulus yz	$(G_{yz})_p$	MPa	5.02

3. NUMERICAL MODELING

In this section, the FE model of the road bridge is firstly described. Secondly, experimental and numerical results from a static test are compared. A modal analysis using the numerical model is thirdly carried out to determine the modes of vibration of the structure.

3.1 Finite Element model

A FE model of the Boyer Bridge is developed in ABAQUS (SIMULIA, 2020), as shown in Figure 1c. Node reduced integration shell elements (S4R) are considered for modelling the orthotropic plate, girders, and cross-beams. The material for the stringers and cross-beams is assumed isotropic with the following values: $\rho_s = 7750$ kg/m^3, $E_s = 200$ GPa and $\nu_s = 0.32$. Whilst the properties of the material for the GFRP plate are stated in Table 1. The grout haunch is not modeled, but a gap of 12.70 mm is provided between the bottom part of the deck and top flanges of the beams to represent the real geometry of the bridge. Additionally, a non-structural mass of 225 kg/m^2 is assigned over the deck to account for the asphalt layer. To model a full composite action, tie constraints are employed between the top flanges of the beams and the corresponding bottom surfaces of the deck. This aims to reproduce a total transfer of the horizontal shear loads between the deck and stringers.

For the boundary conditions, displacements of the bottom flanges of the stringers are constrained in the longitudinal, transversal and vertical (x, y and z) directions at one end of the structure. Whilst, transversal (x) and vertical (z) displacements of the bottom flanges at the another end are constrained.

3.2 Static test

Employing the FE model, the static behavior of the bridge is assessed under the action of a three axle truck. The results obtained from this numerical model are contrasted with the experimental measurements reported by Keelor et al. (2004). The test setup is displayed in Figure 1d, where just the two rear axles appear since the first axle was off the structure during the test. The weights of the axles are 46.37 kN (P3), 41.92 kN (P4), 46.60 kN (P5), and 40.57 kN (P6), and each one acts on a surface of 0.25 m x 0.51 m (Jiang et al., 2013). In Figures 1d-2a, the strain gauges located at the flanges of each beam at 0.305 m from midspan are shown. The strains obtained for the Beam 2 are presented in Figure 2b, where the neutral axis positions measured from the bottom flange are 415 mm and 427 mm considering the experimental and numerical results, respectively.

Comparing the curvature κ in each stringer, the difference between the experimental and numerical values for Beams 1, 2, 3 and 4 are -3 %, +9 %, +18 %, and -17 %, respectively. Since data

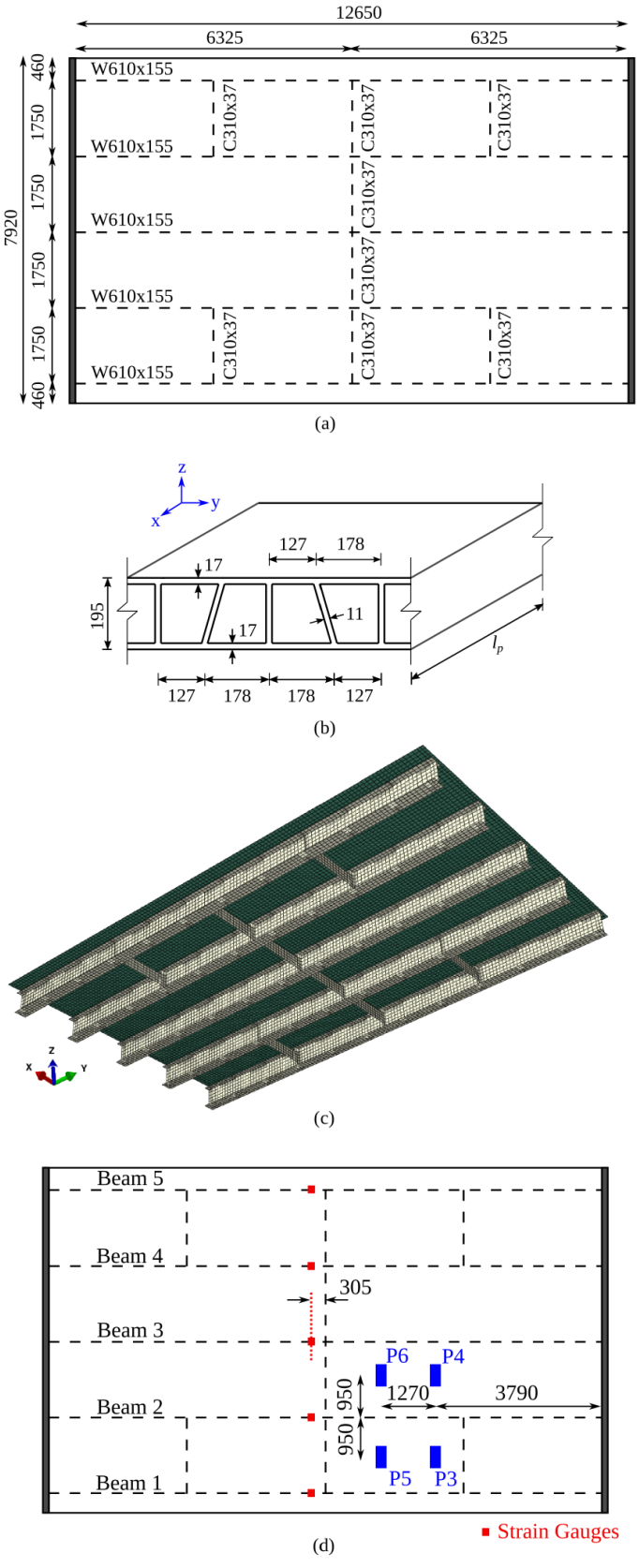

Figure 1. Boyer Bridge: (a) Plan view, (b) GFRP bridge deck, (c) FE model, and (d) Static test. Units in mm

for the Beam 5 was no collected during the test, no comparison is drawn in this element. Based on the obtained results, it is assumed that the developed FE model predicts accurately enough the bridge performance.

3.3 Modal analysis

The dynamic response of a bridge under traffic loads can be anticipated by a simple inspection of its vibration modes, so a modal analysis is performed. Figure 2c presents the first three numerical vibration modes of the GFRP-steel bridge. Mode 1 is a vertical bending mode at 8.87 Hz, Mode 2 is a torsional mode at 11.06 Hz, and Mode 3 is a transverse flexural mode at 20.02 Hz.

Since partial composite action between the deck and the stringers is later studied in this paper, an analysis accounting for this feature is carried out. Rigid connectors are employed instead of the tie constraints mentioned in Section 3.1. Elements type CONN3D2, every 0.61 m, are used to connect nodes of the beams top flanges and the corresponding nodes of the deck in the longitudinal (y) and vertical (z) directions. No constraints are modeled in the lateral (x) direction to represent the reduction in the transfer of the horizontal shear load. The mode shapes are similar to those shown in Figure 2c, but the natural frequencies decrease. The fundamental frequency is 8.36 Hz, whereas values of 10.39 Hz and 18.15 Hz are computed for Modes 2 and 3, respectively.

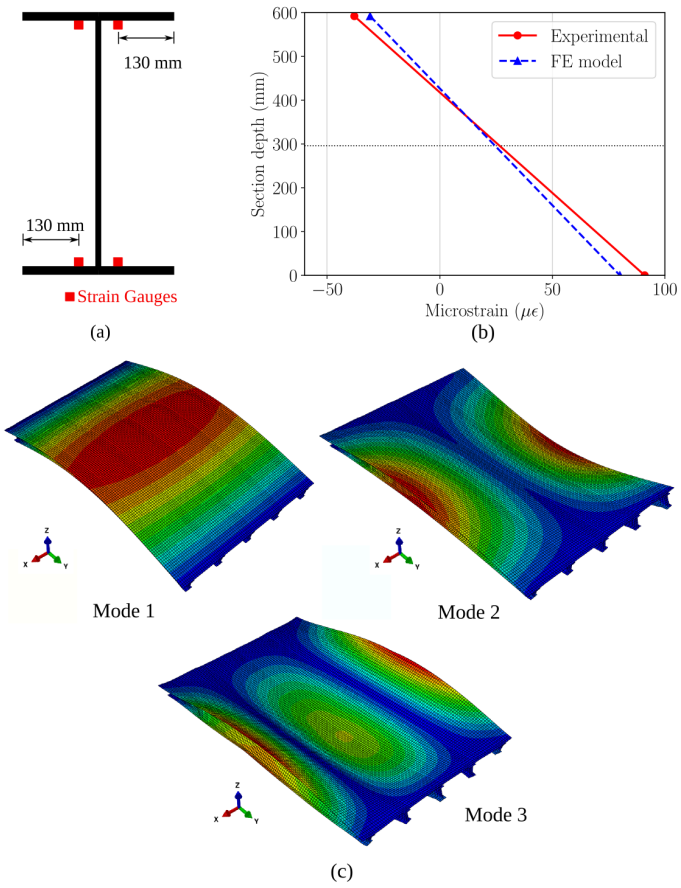

Figure 2. Numerical results: (a) Position of strain gauges in the cross-section of each girder, (b) Strains of Beam 2, and (c) First three vibration modes of the GFRP-steel bridge

4. VEHICLE-BRIDGE INTERACTION

This section presents the generation of roughness profiles to describe the road surface. In addition, the multibody dynamic model of the vehicle is introduced, and the modeling of VBI is explained.

4.1 Road surface

Road roughness is an important source of dynamic excitation in VBI problems, so a proper definition of the pavement irregularities is key for the analysis. In general, road roughness can be represented by an ergodic stationary Gaussian random process described by its Power Spectral Density (PSD). ISO (2016) proposes the expression $G(n_i) = G(n_0)(n/0.1)^{-2}$ for a one-sided PSD, where n is the spatial frequency in cycle/m, and $G(n_0)$ is the spectral roughness coefficient that depends on the road quality in m^3/cycle. A hypothesis of road surface isotropy and homogeneity is assumed in this paper, so parallel profiles of irregularities along the road share statistical properties but they are not the same. Based on Sayers (1988), the profiles for left and right tires can be obtained through the following expressions:

$$z_1(y) = \sum_i^N \sqrt{2G(n_i)\Delta_n}\cos(2\pi n_i y + \phi_i) \tag{7}$$

$$z_2(y) = \sum_i^N \left(\sqrt{2G(n_i)\Delta_n}\cos(2\pi n_i y + \phi_i) + \ldots \right. \\ \left. \ldots \sqrt{(2G(n_i) - G_x(n_i))\Delta_n}\cos(2\pi n_i y + \theta_i)\right) \tag{8}$$

where N is the number of discrete frequencies n_i in range [0.01, 10], Δ_n is the increment between successive frequencies, $G_x(n_i)$ is the cross-PSD, and ϕ_i and θ_i are random phase angles from 0 to 2π.

4.2 Vehicle

A H20-44 truck described in AASHTO (2012) is employed in this study. Eight DOFs are assigned to the whole multibody dynamic model, as displayed in Figure 3. The vehicle consists of individual rigid bodies that represent the box and axles, plus a mass point that reproduces the driver seat. The rigid bodies are connected by linear springs and dashpots to consider the mechanical properties of the suspensions and the behavior of the tires.

The box has 3 DOFs, vertical displacement (z_b), pitch (γ_b), and roll (α_b). Each axle is provided with 2 DOFs, vertical displacement (z_{ra} and z_{fa}), and roll (α_{ra} and α_{fa}). Finally, the driver seat has 1 DOF, vertical displacement (z_d).

Considering Marchesiello et al. (1999), the main properties of the vehicle are: $m_b = 17000$ kg, $m_{ra} = 1000$ kg, $m_{fa} = 600$ kg, $k_{t1} = k_{t2} = 1.57 \times 10^6$ N/m, $k_{t3} = k_{t4} = 7.85 \times 10^5$ N/m, $k_{s1} = k_{s2} = 3.73 \times 10^5$ N/m, $k_{s3} = k_{s4} = 1.16 \times 10^5$ N/m, $c_{t1} = c_{t2} = 200$ N s/m, $c_{t3} = c_{t4} = 100$ N s/m, $c_{s1} = c_{s2} = 3.50 \times 10^4$ N s/m, $c_{s3} = c_{s4} = 2.50 \times 10^4$ N s/m, $I_{\alpha_{ra}} = 600$ kg m^2, $I_{\alpha_{fa}} = 550$ kg m^2, $I_{\alpha_b} = 1.30 \times 10^4$ kg m^2, and $I_{\gamma_b} = 9.00 \times 10^4$ kg m^2. For the driver seat, $m_d = 85$ kg is assumed, whereas the values for the spring ($k_d = 10.51$ kN/m) and the dashpot ($c_d = 876$ Ns/m) are based on Zuo and Nayfeh (2007).

4.3 Interaction

VBI is achieved by means of contact between the bottom nodes of tire elements and the deck surface. This analysis is performed in ABAQUS (SIMULIA, 2020), which provides capabilities to model the vehicle through a multibody system and the structure through finite elements. The vehicle, the bridge, and the interaction phenomenon lead to a nonlinear coupled system, whose global system of equations may be expressed as follows:

$$\begin{bmatrix} \boldsymbol{M_v} & \boldsymbol{0} \\ \boldsymbol{0} & \boldsymbol{M_b} \end{bmatrix} \begin{Bmatrix} \ddot{\boldsymbol{y}}_{\boldsymbol{v}} \\ \ddot{\boldsymbol{y}}_{\boldsymbol{b}} \end{Bmatrix} + \begin{bmatrix} \boldsymbol{C_v} & \boldsymbol{0} \\ \boldsymbol{0} & \boldsymbol{C_b} \end{bmatrix} \begin{Bmatrix} \dot{\boldsymbol{y}}_{\boldsymbol{v}} \\ \dot{\boldsymbol{y}}_{\boldsymbol{b}} \end{Bmatrix} + \begin{bmatrix} \boldsymbol{K_v} & \boldsymbol{0} \\ \boldsymbol{0} & \boldsymbol{K_b} \end{bmatrix} \begin{Bmatrix} \boldsymbol{y_v} \\ \boldsymbol{y_b} \end{Bmatrix} = \begin{Bmatrix} \boldsymbol{F_v} \\ \boldsymbol{0} \end{Bmatrix} + \begin{Bmatrix} \boldsymbol{F_v^c} \\ \boldsymbol{F_b^c} \end{Bmatrix} \tag{9}$$

where $\boldsymbol{M_v}$, $\boldsymbol{C_v}$ and $\boldsymbol{K_v}$ are the mass, damping and stiffness matrices of the vehicle, $\boldsymbol{M_b}$, $\boldsymbol{C_b}$ and $\boldsymbol{K_b}$ are the mass, damping and stiffness matrices of the bridge, $\boldsymbol{F_v}$ is the external force vector of the vehicle due to its self-weight, $\boldsymbol{F_v^c}$ is the force vector applied on the vehicle as consequence of the interaction with the bridge, $\boldsymbol{F_b^c}$ represents its counterpart on the structure, $\ddot{\boldsymbol{y}}_{\boldsymbol{v}}$ and $\ddot{\boldsymbol{y}}_{\boldsymbol{b}}$ are the acceleration response vectors, $\dot{\boldsymbol{y}}_{\boldsymbol{v}}$ and $\dot{\boldsymbol{y}}_{\boldsymbol{b}}$ are the velocity response vectors, and $\boldsymbol{y_v}$ and $\boldsymbol{y_b}$ are the displacement response vectors of the vehicle and bridge, respectively.

5. SENSITIVITY ANALYSIS

A sensitivity analysis is presented in this section to identify the most relevant mechanical properties of the orthotopic plate on the numerical response of the GFRP-steel structure. Additionally, the response of the hybrid road bridge is assessed when some properties of the deck are modified.

5.1 Identification of relevant properties

Focusing on the natural frequencies of the hybrid bridge, a global sensitivity analysis aiming to identify the most relevant material properties of the orthotropic plate is performed herein. The properties of the plate $\left((E_x)_p, (E_y)_p, \nu_{xy}, (G_{xy})_p, (G_{xz})_p, \text{and } (G_{yz})_p\right)$ are assumed to be described by a two-parameter Weibull probability distribution based on Alqam et al. (2002). Mean values for the distribution of each property are taken from Table 1, and a coefficient of variation of 10 % is considered. Also, the Latin Hypercube Method is used to generate 500 multivariate stochastic samples of the mechanical properties. Parameters related to boundary conditions, steel elements and density of the materials are not considered in this analysis.

Figure 4 shows the results through the Spearman correlation coefficient matrix, where values between $[-0.2, +0.2]$ are excluded for a better visualization. From the correlation matrix, it is seen that the longitudinal modulus $(E_y)_p$, the transverse modulus $(E_x)_p$, and the shear modulus $(G_{xy})_p$ of the deck are the most influential factors to obtain the natural frequencies of the FE model of the bridge.

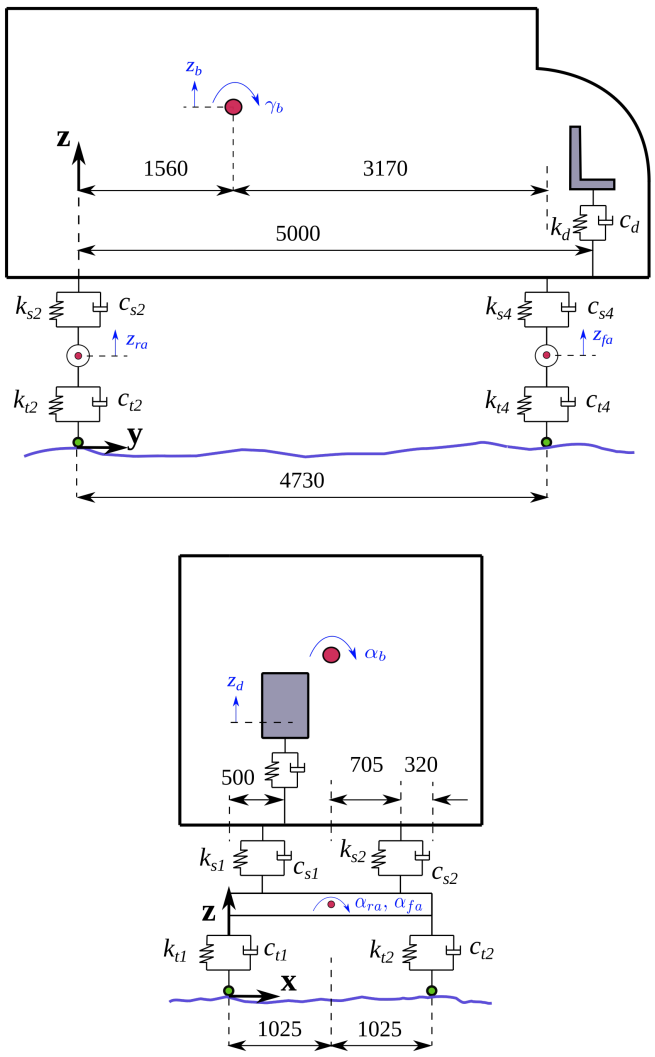

Figure 3. Side and rear view of the multibody dynamic model of an AASHTO H20-44 truck. Units in mm

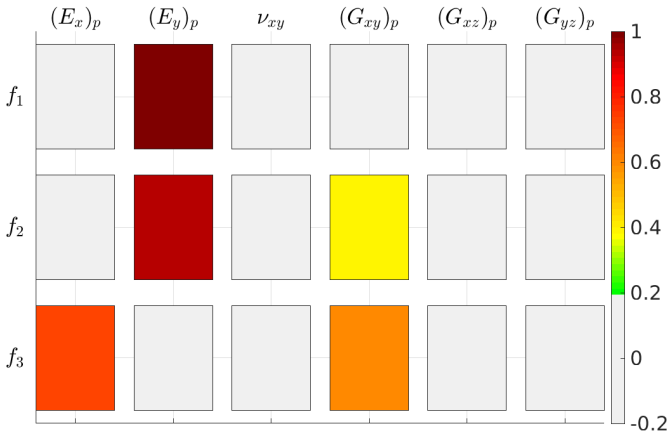

Figure 4. Spearman correlation matrix of parameters that correspond to the orthotropic plate in a fully composite model of the bridge

5.2 Variation of relevant parameters

Based on the previously obtained results, a parametric study varying $(E_y)_p$, $(E_x)_p$, and $(G_{xy})_p$ is carried out hereby. The mean value of each property (Table 1) is modified 10 % in a range from 80 % to 120 %. For the analyses, the H20-44 truck is aligned with the center line of Beam 2 (Figure 5a), and a velocity of 60 km/h is

considered.

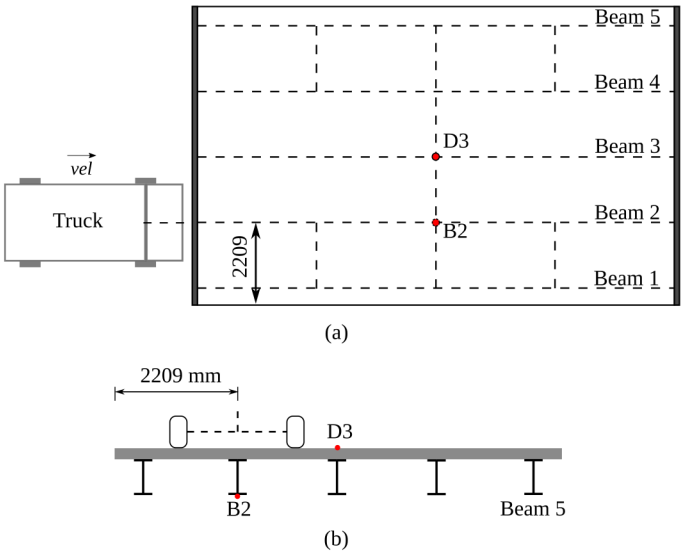

Figure 5. Truck alignment: (a) Plan view, and (b) Front view

The displacement response at the midspan bottom of Beam 2 (point B2) is calculated, and the acceleration response at the deck center (point D3) is obtained. In Figure 5b, the points where the structural response is computed are shown. A very good quality surface of the pavement (Class A according to ISO (2016)) is considered for the simulations. For the sake of statistical significance, ten synthetic pairs of profiles, whose irregularities are sampled every 2 cm, are generated. Equations (7)-(8) are used for the definition of the road roughness, adopting $G(n_o) = 16\times\ 10^{-6}$ and 2000 spatial frequencies between 0.01 m^{-1} and 10 m^{-1}. To obtain $G_x(n_i)$, the procedure described by Oliva et al. (2013) is employed. To ensure that the truck presents a stable response due to the pavement irregularities before entering the bridge, the vehicle is considered to start traveling with its rear tires located at -50 m of the longitudinal model coordinate ($y = 0$ corresponds to bridge entrance). The calculation is also performed until the rear tires are 35 m after the exit abutment. Hence, the vehicle runs a distance equal to 50+L_b+35 m.

Since the implications full and partial composite actions between the deck and the stringers are also studied, 300 dynamic analyses are carried out in total. To solve the system of differential equations (Equation (9)), the HHT-α implicit integration method is used, a constant time step of 0.001 s is set, and a Rayleigh damping of 1 % is adopted.

In Figure 6, the computed results are presented. The graphs show the average of the peak responses (mean of absolute maximum values), displacement at point B2 and acceleration at point D3, when the parameters of the orthotropic plate change. The colored bands in the plots represent the peak responses obtained after using the ten set of road roughness profiles. As expected, higher displacements and vibration levels are obtained for the partially composite model of the bridge in comparison with the fully composite one. Table 2 presents the dynamic responses for both models of the GFRP-steel bridge. These results are the average of the ten peak responses obtained when the value of the analyzed property is multiplied by 0.8 and 1.2, respectively.

By varying $\pm 20\,\%$ the relevant properties of the orthotropic plate in the fully composite model, the average of the peak responses changes up to:

- Displacement: 1 %, 12 %, and 1 % for the variation of $(E_x)_p$, $(E_y)_p$, and $(G_{xy})_p$, respectively.
- Acceleration: 2 %, 6 %, and 2 % for the variation of $(E_x)_p$, $(E_y)_p$, and $(G_{xy})_p$, respectively.

Whilst in the partially composite bridge, modifying $\pm 20\,\%$ the equivalent properties of the deck system lead to the following variations of the average the peak responses:

- Displacement: 1 %, 11 % and 1 % for the variation of $(E_x)_p$, $(E_y)_p$ and $(G_{xy})_p$, respectively.
- Acceleration: 2 %, 6 % and 2 % for the variation of $(E_x)_p$, $(E_y)_p$ and $(G_{xy})_p$, respectively.

Table 2. Bridge response when the vehicle speed is 60 km/h

Parameter	Value	Full		Partial	
		Disp.	Accel.	Disp.	Accel.
	(GPa)	(mm)	(m/s^2)	(mm)	(m/s^2)
$(E_x)_p$	12.51	-3.66	1.51	-3.94	2.10
	18.76	-3.63	1.64	-3.90	2.17
$(E_y)_p$	5.73	-3.90	1.69	-4.15	2.14
	8.60	-3.46	1.53	-3.73	2.16
$(G_{xy})_p$	5.16	-3.68	1.56	-3.94	2.15
	7.74	-3.62	1.63	-3.90	2.15

6. DYNAMIC RESPONSE

In this section, the Dynamic Amplification Factor (DAF) of the GFRP-steel bridge is discussed varying the truck speed and the quality of the road surface. Also, the acceleration response of the driver seat in the vehicle is presented.

For the numerical analyses, the considerations mentioned in the previous section are adopted. Also, the H20-44 truck is assumed to move at 40, 60, 80 and 100 km/h, and two road surfaces are defined. Hence, values of $G(n_o)$ equal to 16×10^{-6} (road A, very good quality) and 256×10^{-6} (road C, regular quality) are employed. As ten pair of profiles are again generated for statistical significance, 160 simulations are carried out.

6.1 Dynamic amplification factor

The results at the bottom flange of the Beam 2 (point B2 in Figure 5) when the vehicle runs over the bridge at 100 km/h are presented in Figures 7a-b. The colored bands shown in these graphs represent the dispersion of response displacements obtained from the ten set of roughness profiles. The width of this band corresponds to the minimum and maximum displacements calculated.

In the plots, results for a perfectly flat surface are also represented together with the maximum static displacement. It is clear that the response increases by worsening the quality of the road surfaced. Similarly, the reduction of composite action in the hybrid road bridge impacts negatively in the structural response.

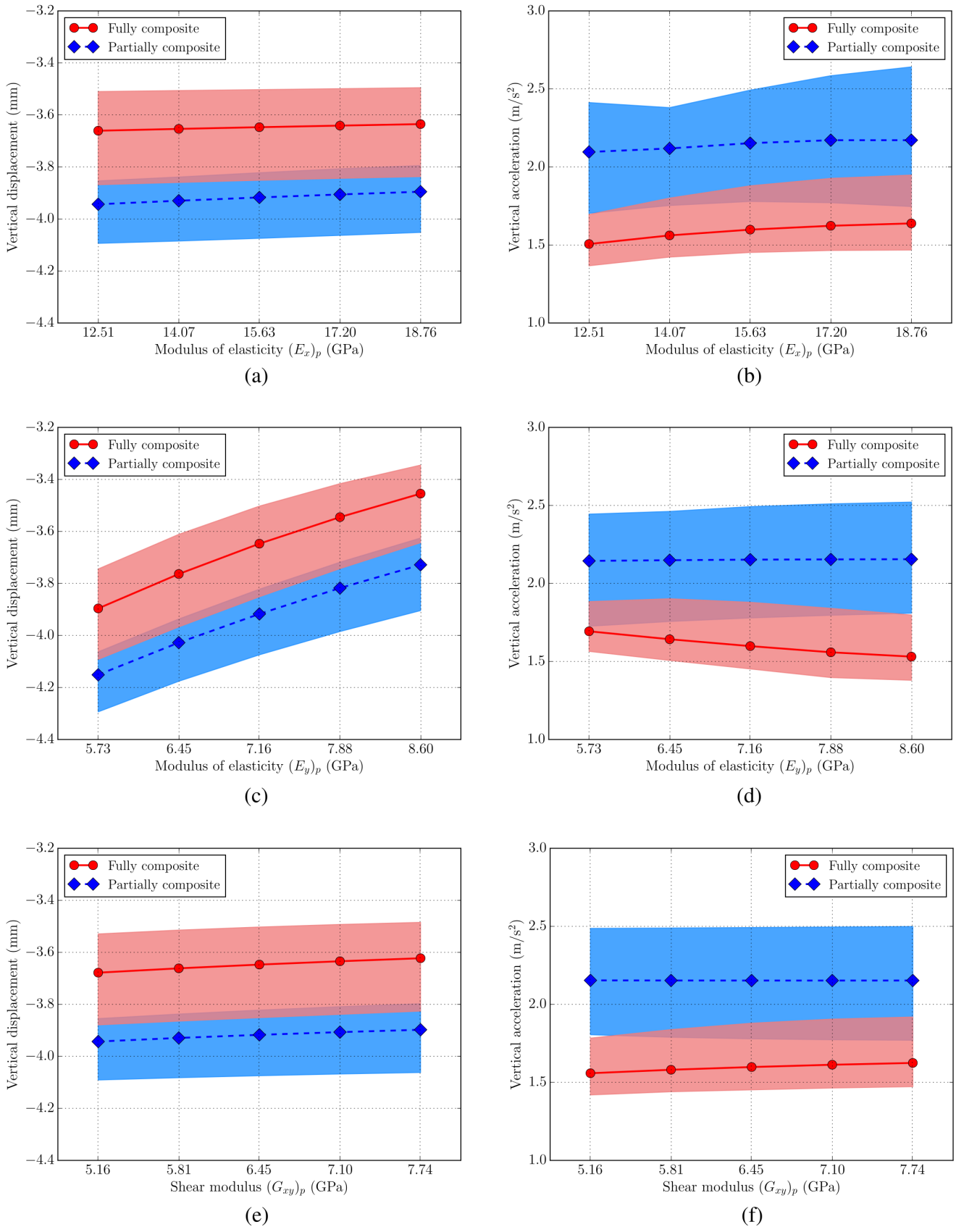

Figure 6. Truck running at 60 km/h in a road Class A: (a) Displacement at B2 varying $(E_x)_p$, (b) Acceleration at D3 varying $(E_x)_p$, (c) Displacement at B2 varying $(E_y)_p$, (d) Acceleration at D3 varying $(E_y)_p$, (e) Displacements at B2 varying $(G_{xy})_p$, and (f) Acceleration at D3 varying $(G_{xy})_p$

Considering that the DAF is defined as:

$$\text{DAF} = \frac{R_d}{R_s} \tag{10}$$

where R_d and R_s are the maximum dynamic and static responses of the bridge at a specific location, Figure 7c presents the maximum DAF at point B2 for different truck speeds.
Maximum results among the ten set of profiles, depending on the road class and composite action of the bridge, are shown. The DAF for a perfectly flat surface is also represented. Generally, in the graph, the higher the vehicle speed, the higher the maximum DAF. As expected, a higher bridge response is also obtained when the composite action is reduced, and the worse results are obtained when the partially composite model is assessed considering a poor quality of the road surface.

6.2 Driver seat

The vertical accelerations at the seat of the truck are analyzed herein to study the dynamic effects on the driver. Figure 8a shows the computed response for one set of road Class A synthetic profiles when the vehicle runs at 100 km/h. To assess the bridge flexibility influence, results of the truck on the bridge and on a rigid road platform are compared under the same road surface conditions. From this plot, it can be firstly seen that the degree of composite action in the model is not relevant on the driver comfort since similar accelerations are obtained. Additionally, the structure flexibility slightly modifies the response at the driver seat but it is not a key factor given the short span of the bridge.
In Figure 8b, the average of the peak vertical acceleration at the driver seat for different vehicle speeds is displayed. In this graph, acceleration when the truck runs over a pavement without irregularities (perfect road) is also included. It is clear that the road quality and the vehicle speed impact largely the peak response at the driver seat.

7. CONCLUSIONS

In this study, the dynamic behavior of a GFRP-steel road bridge has been assessed by carrying out an analysis considering VBI. The influence of the properties of a multicellular GFRP deck, modeled as an orthotropic plate, on the bridge response has been investigated considering the degree of composite action between the deck and the girders, the road roughness, and a multibody dynamic model for the vehicle. Based on the obtained results, the following conclusions may be drawn:

- The longitudinal modulus of elasticity $(E_y)_p$, transverse modulus of elasticity $(E_x)_p$, and the shear modulus $(G_{xy})_p$ are the most influential properties of the orthotropic plate on the dynamic performance of the hybrid road bridge.
- Modifying $\pm 20\,\%$ the mean values of $(E_y)_p$, $(E_x)_p$, and $(G_{xy})_p$ does not lead to significant differences in the final computed response of the GFRP-steel bridge.
- Numerical results confirmed previous observations about the importance of achieving full composite action between the girders and deck to control high dynamic responses in hybrid bridges.

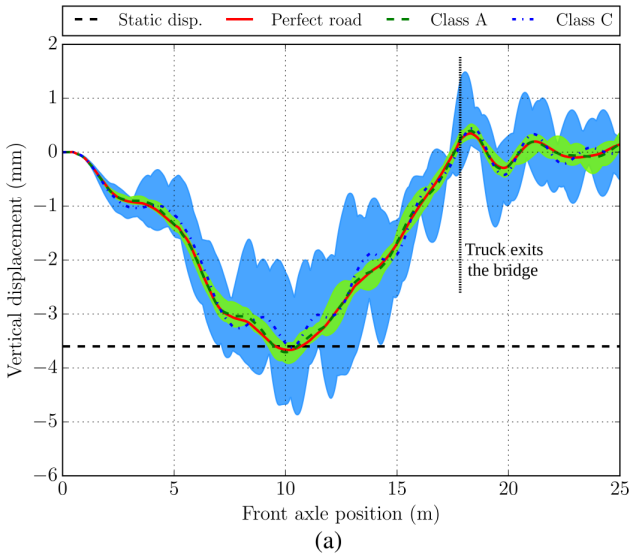

(a)

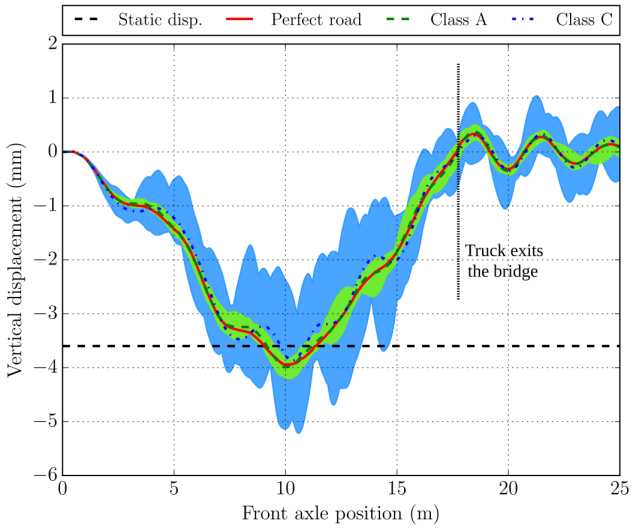

(b)

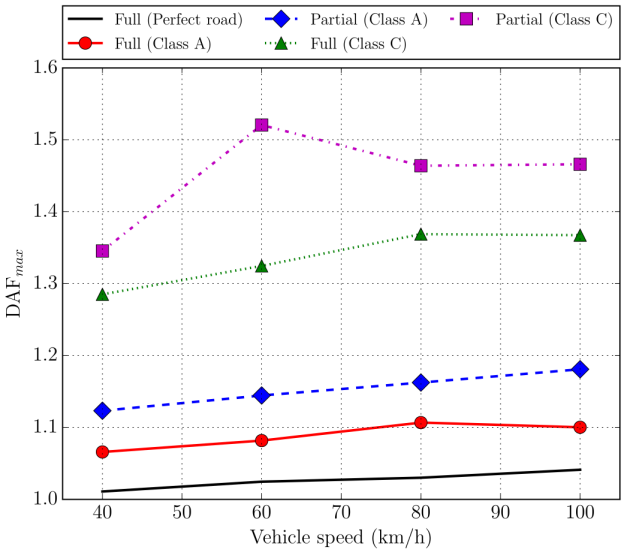

(c)

Figure 7. Vertical displacement of point B2: (a) Fully composite model when the vehicle speed is 100 km/h, (b) Partially composite model when the truck velocity is 100 km/h, and (c) Maximum DAF for different vehicle speeds

- In terms of the DAF, deterioration of road surface is more important than reduction of composite action. Hence, a good construction and a proper maintenance are of great importance for this kind of road bridge due to its dynamic sensitivity.
- Road roughness is more relevant than the degree of composite action in regard to dynamic effects on the driver.

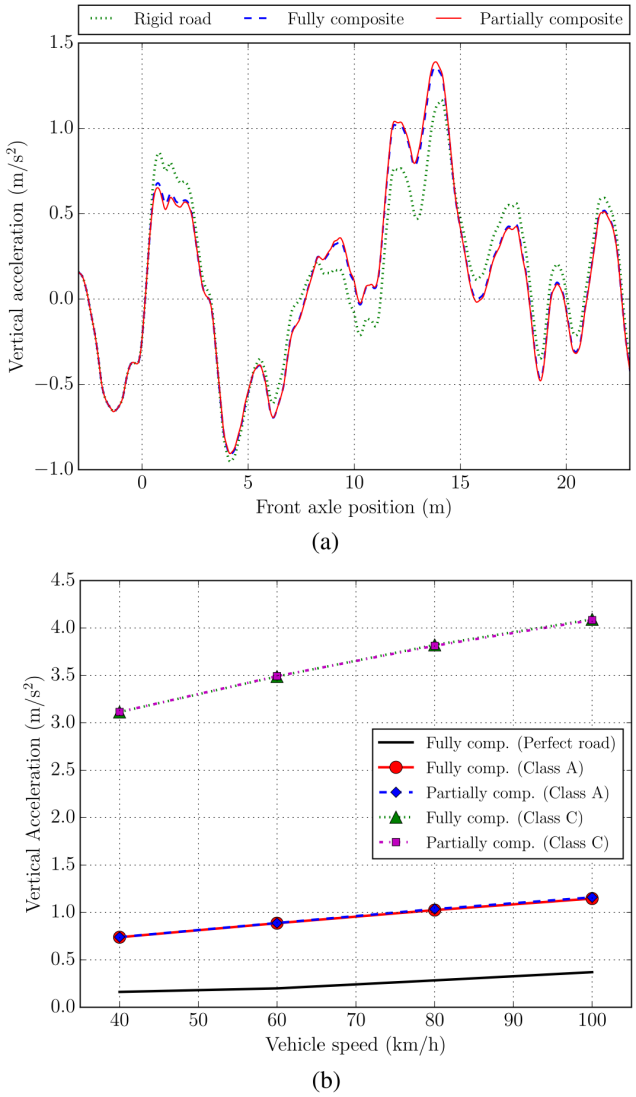

Figure 8. Response of the driver seat: (a) Vertical acceleration when the truck speed is 100 km/h in a road Class A, and (b) Average of peak acceleration for different vehicle speeds

ACKNOWLEDGEMENTS

The authors acknowledge the grant PID2021-127627OB-I00 funded by Ministerio de Ciencia e Innovación, Agencia Estatal de Investigación and 10.13039/501100011033 FEDER, European Union. Christian Gallegos-Calderón expresses his gratitude to Secretaría de Educación Superior, Ciencia, Tecnología e Innovación de Ecuador (SENESCYT) for the doctoral scholarship CZ02-000167-2018.

REFERENCES

AASHTO (2012). *AASHTO LRFD Bridge Design Specifications*. American Association of State Highway and Transportation Officials

Alqam, M., Bennett, R. M., and Zureick, A. H. (2002). Three-parameter vs. two-parameter Weibull distribution for pultruded composite material properties. *Composite Structures*, *58*(4), 497–503. https://doi.org/10.1016/S0263-8223(02)00158-7

Aluri, S., Jinka, C., and GangaRao, H. (2005). Dynamic Response of Three Fiber Reinforced Polymer Composite Bridges. *Journal of Bridge Engineering*, *10*(6), 722–730. https://doi.org/10.1061/(ASCE)1084-0702(2005)10:6(722)

ISO (2016). *ISO 8608: Mechanical Vibrations - Road Surface Profiles - Reported Of Measured Data*. International Organization for Standardization, Geneva.

Jiang, X., Ma, Z., and Song, J. (2013). Effect of shear stud connections on dynamic response of an FRP deck bridge under moving loads. *Journal of Bridge Engineering*, *18*(7), 644–652. https://doi.org/10.1061/(ASCE)BE.1943-5592.0000401

Joint Research Centre (2016). *Prospect for new guidance in the design of FRP*. European Commission, Ispra. https://publications.jrc.ec.europa.eu/repository/handle/JRC99714

Keelor, D., Luo, Y., Earls, C., and Yulismana, W. (2004). Service load effective compression flange width in fiber reinforced polymer deck systems acting compositely with steel stringers. *Journal of Composites for Construction*, *8*(4), 289–297. https://doi.org/10.1061/(ASCE)1090-0268(2004)8:4(289)

Kim, Y. (2019). State of the practice of FRP composites in highway bridges. *Engineering Structures*, 179, 1–8. https://doi.org/10.1016/j.engstruct.2018.10.067

Lee, S., Hong, K., and Park, S. (2010). Current and Future Applications of Glass-Fibre-Reinforced Polymer Decks in Korea. *Structural Engineering International*, *20*(4), 405–408. https://doi.org/10.2749/101686610793557672

Mara, V. and Haghani, R. (2015). Review of FRP decks: structural and in-service performance. *Proceedings of the Institution of Civil Engineers - Bridge Engineering*, *168*(4), 308–329. https://doi.org/10.1680/bren.14.00009

Mara, V., Haghani, R., and Harryson, P. (2014). Bridge decks of fibre reinforced polymer (FRP): A sustainable solution. *Construction and Building Materials*, *50*, 190–199. https://doi.org/10.1016/j.conbuildmat.2013.09.036

Marchesiello, S., Fasana, A., Garibaldi, L., and Piombo, B. (1999). Dynamics of multi-span continuous straight bridges subject to multi-degrees of freedom moving vehicle excitation. *Journal of Sound and Vibration*, *224*(3), 541–561. https://doi.org/10.1006/jsvi.1999.2197

Oliva, J., Goicolea, J., Antolín, P., and Astiz, M. (2013). Relevance of a complete road surface description in vehicle-bridge interaction dynamics. *Engineering Structures*, 56, 466–476. https://doi.org/10.1016/j.engstruct.2013.05.029

Qiao, P., Davalos, J. F., and Brown, B. (2000). A systematic analysis and design approach for single-span FRP deck/stringer bridges. *Composites Part B: Engineering*, *31*(6-7), 593–609. https://doi.org/10.1016/S1359-8368(99)00044-X

Resins, B. D. D. C. (2009). LCA Composietbrug Eindrapport (2e versie). Technical report, BECO Group, Rotterdam.

Sayers, M. (1988). Dynamic terrain inputs to predict structural integrity of ground vehicles. Technical report, University of Michigan, Transportation Research Institute, Michigan.

SIMULIA (2020). *Abaqus 2020 Analysis User's Guide*. Dassault Systèmes Simulia Corporation.

Wan, B., Rizos, D., Petrou, M., and Harries, K. (2005). Computer simulations and parametric studies of GFRP bridge deck systems. *Composite Structures*, *69*(1), 103–115. https://doi.org/10.1016/j.compstruct.2004.05.012

Zhang, Y., Cai, C., Shi, X., and Wang, C. (2006). Vehicle-Induced Dynamic Performance of FRP versus Concrete Slab Bridge. *Journal of Bridge Engineering*, *11*(4), 410–419. https://doi.org/10.1061/(ASCE)1084-0702(2006)11:4(410)

Zuo, L. and Nayfeh, S. (2007). H_2 optimal control of disturbance-delayed systems with application to vehicle suspensions. *Vehicle System Dynamics*, *45*(3), 233–247. https://doi.org/10.1080/00423110600884288

BIOGRAPHIES

Christian, Gallegos-Calderón. Civil Engineer from Escuela Politécnica Nacional. Master of Engineering, Structures from The University of Melbourne. PhD in Structural Engineering from Universidad Politécnica de Madrid (UPM). He has carried out activities related to the analysis, design, construction, and structural behaviour assessment of buildings and bridges. Additionally, he has worked for Ecuadorian and Spanish universities. Research interests: bridge dynamics, FRP structures, and vibration control systems.

Javier, Oliva-Quecedo. Civil Engineer from UPM. PhD in Structural Engineering from UPM. He has authored several conference and scientific journal papers. He has participated in several research projects with companies and administrations. Also, he has given lectures at UPM and Saint Louis University-Madrid. Currently, he collaborates with AR2V, an independent firm specialising in the design of bridges and other structures. Research interests: bridge design, structural dynamics, and biomechanics.

M. Dolores, Pulido. Civil Engineer from UPM. PhD in Structural Engineering from Universitat Politècnica de Catalunya. She has been lecturer in undergraduate and postgraduate programs at different Spanish universities. She is Head Scientist at Eduardo Torroja Institute for Construction Sciences (IETcc-CSIC), belonging to the Spanish National Research Council. She is also Professor at UPM. Research interests: FRP structures, structural strengthening with FRP, deployable structures, and Computational Mechanics.

José, Goicolea. Civil Engineer from UPM. PhD in Engineering from University of London. He is full professor at the School of Civil Engineering-UPM since 1993. He has authored more than 100 conference and scientific journal papers, and has developed around 60 research projects for companies and administrations. He is the Chair of the Department of Continuum Mechanics and Theory of Structures at the School of Civil Engineering and member of the General Council of the International Association for Computational Mechanics. Research interests: structural dynamics and cardiovascular biomechanics.